

# Pathology of Echinococcosis

## A Morphologic and Immunohistochemical Study on 138 Specimens With Focus on the Differential Diagnosis Between Cystic and Alveolar Echinococcosis

Michael Reinehr,\* Charlotte Micheloud,† Felix Grimm, PhD,‡ Philipp A. Kronenberg, MSc,‡§ Johannes Grimm,|| Annika Beck, MD,|| Juliane Nell,|| Cordula Meyer zu Schwabedissen, MD,¶ Eva Furrer, PhD,† Beat Müllhaupt, MD,¶ Thomas F.E. Barth, MD,|| Peter Deplazes, DVM,‡ and Achim Weber, MD\*#

**Abstract:** Infection of humans by the larval stage of the tapeworms *Echinococcus granulosus sensu lato* or *Echinococcus multilocularis* causes the life-threatening zoonoses cystic echinococcosis (CE) and alveolar echinococcosis (AE). Although cystic liver lesions are a hallmark of both diseases, course, prognosis, and patients' management decisively differ between the two. The wide and overlapping spectrum of morphologies and the limited availability of ancillary tools are challenges for pathologists to reliably diagnose and subtype echinococcosis. Here, we systematically and quantitatively recorded the pathologic spectrum in a clinically and molecularly defined echinococcosis cohort (138 specimens from 112 patients). Immunohistochemistry using a novel monoclonal antibody (mAbEmG3) was implemented, including its combined application with the mAbEm2G11. Six morphologic criteria sufficiently discriminated between CE and AE: size of smallest (CE/AE:

$>2/\leq 2$  mm) and largest cyst (CE/AE:  $>25/\leq 25$  mm), thickness of laminated layer (CE/AE:  $>0.15/\leq 0.15$  mm) and pericystic fibrosis (CE/AE:  $>0.6/\leq 0.6$  mm), striation of laminated layer (CE/AE: moderate-strong/weak), and number of cysts (CE/AE:  $\leq 9/>9$ ). Combined immunohistochemistry with mAbEm2G11 (*E. multilocularis* specific) and mAbEmG3 (reactive in AE and CE) was equally specific as and occasionally more sensitive than polymerase chain reaction. On the basis of these findings, we developed a diagnostic algorithm for the differential diagnosis of echinococcosis. In summary, we have not only identified the means to diagnose echinococcosis with greater certainty, but also defined morphologic criteria, which robustly discriminate between CE and AE. We expect our findings to improve echinococcosis diagnostics, especially of challenging cases, beneficially impacting the management of echinococcosis patients.

**Key Words:** echinococcosis, differential diagnosis, morphology, immunohistochemistry, diagnostic algorithm, *Echinococcus multilocularis*, *Echinococcus granulosus sensu lato*

(*Am J Surg Pathol* 2020;44:43–54)

From the \*Department of Pathology and Molecular Pathology; ¶Clinics of Hepatology and Gastroenterology, University of Zurich and University Hospital Zurich; †Epidemiology, Biostatistics and Prevention Institute; ‡Institute of Parasitology; #Institute of Molecular Cancer Research, University of Zurich, Zurich; §Graduate School for Cellular and Biomedical Sciences, University of Bern, Bern, Switzerland; and ||Institute of Pathology, University of Ulm, Ulm, Germany.

M.R. and A.W.: concept and design of study. A.B., J.N., J.G., T.F.E.B., C.M.z.S., and B.M.: providing tissue biopsies and related clinical information. P.A.K. and P.D.: antibody development. F.G.: molecular testing. M.R. and A.W.: evaluation of histology and immunohistochemistry. M.C. and E.F.: statistical analysis. M.R. and A.W.: preparation of figures and writing of the manuscript. All authors read and agreed to the manuscript.

**Conflicts of Interest and Source of Funding:** Supported by the basic funding by the Medical Faculty Zurich to A.W. The authors have disclosed that they have no significant relationships with, or financial interest in, any commercial companies pertaining to this article.

**Correspondence:** Achim Weber, MD, Department of Pathology and Molecular Pathology, University Zurich and University Hospital Zurich, Schmelzbergstrasse 12, Zurich 8091, Switzerland (e-mail: achim.weber@usz.ch).

Supplemental Digital Content is available for this article. Direct URL citations appear in the printed text and are provided in the HTML and PDF versions of this article on the journal's website, www.ajsp.com.

Copyright © 2019 Wolters Kluwer Health, Inc. All rights reserved.

With >1 million people infected worldwide, echinococcosis is a globally occurring parasitic disease with a significant health burden.<sup>1,2</sup> It is listed among the neglected tropical diseases recognized by the World Health Organization.<sup>3</sup> Echinococcosis is more prevalent in rural areas, in particular, of resource-poor countries, but, recently, shifting more and more into urban areas.<sup>4</sup> Local transmission is also well documented in North America including the United States, with an increase in incidence observed, especially for alveolar echinococcosis (AE), not only in the United States but also in Central Europe.<sup>5–7</sup> Hence, there is increasing awareness of echinococcosis as a potentially emerging threat to humans in rural and in inner-city areas all over the world.

Humans are infected by the eggs of *Echinococcus* spp. when exposed to infected definitive hosts (eggs on animal hair), via the contaminated environment (hands-mouth

transmission), or by consuming contaminated food (vegetables, water),<sup>8</sup> and present a dead end for the parasitic infection cycle. Echinococcosis is a disease caused by different *Echinococcus* spp., manifesting either in a cystic, polycystic, or alveolar form.<sup>9</sup> Cystic echinococcosis (CE; alias unilocular echinococcosis) is caused by the larval (metacestode) stage of *Echinococcus granulosus sensu lato* (referred in this paper as *E. granulosus*), AE (alias alveolar hydatid disease or multilocular echinococcosis) is caused by *Echinococcus multilocularis*, and polycystic echinococcosis (alias polycystic hydatid disease or neotropical echinococcosis) by *Echinococcus vogeli* or *Echinococcus oligarthra*, both of which only rarely affect humans. In echinococcosis, liver and less frequently lungs are primarily affected, but manifestations of the disease can occur in virtually any organ system.<sup>10</sup>

The clinical presentation of echinococcosis in humans ranges from asymptomatic to severe disease depending on the location and species of parasites and stage of the disease.<sup>10</sup> Although an expansive growth is typical for CE, AE is characterized by an infiltrative, cancer-like growth, frequently invading and destroying tissue, with extension beyond organ borders or distant spread. Mainly due to this aggressive growth, AE may take a fatal course.<sup>9</sup> The diagnosis of echinococcosis is usually made in a multimodal approach, taking advantage of a combination of imaging techniques including ultrasonography, magnetic resonance imaging, and computed tomography scans,<sup>11,12</sup> and serologic tests such as enzyme-linked immunosorbent assay (ELISA) and Western blotting. Confirmation of probable cases, as defined by the World Health Organization,<sup>13</sup> can be achieved by nucleic acid–based analysis (polymerase chain reaction [PCR]/sequencing) or by histopathologic analysis of tissue samples (biopsy, surgical material, autopsy, and fine-needle aspirates).<sup>14,15</sup> Currently available serologic tests for AE reach high sensitivity and specificity with clinical samples from European patients; however, even a combination of several tests showed strongly reduced sensitivities dependent on the stage of AE and were greatly reduced in early and very small lesions.<sup>16</sup> Finally, histopathology, occasionally supplemented with DNA analyses and/or immunohistochemistry (IHC) if available, is the gold standard of diagnosis.<sup>17,18</sup>

Pathologists are faced with tissue specimen containing the metacestode stage of *Echinococcus* spp. not only in cases clinically suspicious of echinococcosis, but also in cases of liver lesions suspicious of a neoplastic lesion. The literature on the histopathology of echinococcosis includes articles and textbook chapters involving histopathology, among other topics. Although the main features are listed, a rigorous comparison is still lacking. In addition, several comments on specific characteristics do not withstand our observations in daily diagnostics—for example, the notion that protoscolices are not observable in AE.<sup>4,17,19,20</sup> This imprecision can lead to substantial uncertainty of diagnosis, possibly preventing the correct subclassification of echinococcosis.

This prompted us to systematically and comprehensively analyze the histopathology of echinococcosis with the aim to define differential criteria. Furthermore, we tested the informative value of two monoclonal antibodies (mAbs)

produced against *E. multilocularis* metacestode antigens for application in daily pathology practice.

## MATERIALS AND METHODS

Samples were identified from the archives of the Department of Pathology and Molecular Pathology, University Hospital Zurich (USZ), between 1997 and 2018. All cases were reevaluated for this study. Clinical information was retrieved from the USZ *Echinococcus* register. This study was reviewed and approved by the internal review board of the University Hospital Zurich and the Cantonal Ethics Committee of Zurich, Switzerland (KEK-ZH-Nr. 2015-0498).

### Antibody Production

Two immunohistochemical stainings (IHC-S) were applied in this study as a screening strategy for infection with *Echinococcus* spp. The first IHC-S with the immunoglobulin (Ig) G1 mAbEm2G11 was directed against a mucin-type Em2 glycoprotein specific for *E. multilocularis*.<sup>17,21,22</sup> The second IHC-S with the IgM mAbEmG3 was directed against an antigen, which has not been characterized yet. Both mAbs are in vitro produced mAbs from a mouse hybridoma cell line, as described in detail.<sup>22</sup> The mAbEmG3 was produced in the same fusion as the mAbEm2G11, but was not further used because of cross-reactivity to *E. granulosus* metacestode antigens. For this study, both antibodies have been reevaluated for their specificity against a panel of helminths' antigens (for details, see Supplement 1—Table, Supplemental Digital Content 1, <http://links.lww.com/PAS/A841>).

### Characterization of the Specificity of the mAbs mAbEm2G11 and mAbEmG3 in ELISA Using Native *Echinococcus* spp. and Antigens of Other Helminths

ELISA was performed in principal, as described by Schweiger et al<sup>14</sup> mAb were produced in vitro by hybridoma cell cultivation. Supernatants containing the mAbs were added in a dilution of 1:2 in ELISA buffer (PBS [pH 7.2] containing 0.02% [wt/vol] Na<sub>3</sub>N, 0.05% [wt/vol] bovine hemoglobin, and 0.3% [v/v] Tween-20 [PBS-T]). Mouse serum of an experimentally infected animal with AE was diluted 1:100. Anti-mouse IgG (whole molecule)-alkaline phosphatase conjugate (Sigma-Aldrich, A3562) was used in a dilution of 1:10,000 in PBS-T. ELISA substrate readout was performed after 20 minutes at 405 nm (OD<sub>405</sub>) with a reference wavelength of 630 nm. The mAbDi36/1, directed to *Dirofilaria immitis* and *Dirofilaria repens* adult somatic and E/S antigens,<sup>23</sup> was used as a negative control antibody for *Echinococcus* spp. epitopes. Native *Echinococcus* spp. antigens were prepared, as previously described.<sup>14</sup> Antigens of other helminths were prepared, as described by Deplazes and Gottstein.<sup>22</sup> The mouse serum from a BALB/c mouse infected with 500 viable eggs of *E. multilocularis* with liver AE was used for the documentation of the antigenicity of the antigens applied (animal experiment authorized by the

Cantonal Veterinary Office of Zurich, Switzerland (permission no. 294/2014)).

The mAbEmG3 and the mAbEm2G11 are available on request from Peter Deplazes at the Institute of Parasitology, University of Zurich, Switzerland.

## Histology, Histochemical Stains, IHC, and Imaging

Histologic, histochemical, and IHC-S and digitalization for virtual microscopy were performed, as previously described with slight modifications.<sup>24,25</sup> Briefly, tissues were fixed in 4% paraformaldehyde and paraffin embedded. Tissue sections (2 to 3  $\mu$ m thickness) were stained with hematoxylin and eosin (H&E), elastica van Gieson, periodic acid-Schiff, or with mAbEmG3 or characterization of the mAbEm2G11. Immunohistochemical staining with both mAbs comprised 30 minutes pretreatment at 100°C with TrisEDTA borat (pH 9.0), dilution 1:200 (mAbEm2G11) and 1:1000 (mAbEmG3), respectively, incubation for 30 minutes (Leica Bond-III), and detection with Bond Polymer Refine Detection Kit. Histologic and IHC slides were digitalized for virtual microscopy, archiving, and image preparation for figures, using a Nano Zoomer C9600 Virtual Slide Light microscope scanner by Hamamatsu using NDP, View Software.

## Genetic Analyses

Species-specific PCRs targeting the mitochondrial 12S rRNA gene were performed on DNA isolated from FFPE tissue samples according to Stieger et al<sup>26</sup> for *E. multilocularis* and according to Stefanic et al,<sup>27</sup> or—if the first PCR was negative—according to Trachsel et al<sup>28</sup> for *E. granulosus*. Amplicons were sequenced by a private company service (Synergene Biotech GmbH, Schlieren, Switzerland).

## Statistical Analyses

To assess the agreement of IHC-S and PCR (gold standard) for discrimination of *Echinococcus* spp., the calculation of Cohen  $\kappa$  was recommended.<sup>29</sup> As this calculation was not possible due to perfect agreement, we relied on a simulation approach to assess how likely perfect agreement is in different scenarios. For the continuous morphologic criteria, receiver operating characteristic (ROC) curves were plotted, and the area under the curve was calculated as a measure for the discriminative power of the criteria between an infection with *E. multilocularis* and an infection with *E. granulosus*. Higher area under the curves indicate better diagnostic power.<sup>30</sup> Optimal cutpoints were determined from the ROC curve by maximization of the sum of sensitivity and specificity. For the binary morphologic criteria, sensitivity and specificity were calculated as measures for the discriminative power between CE and AE. A criterion having both specificity and sensitivity > 0.85 was considered a good diagnostic test. For defining a diagnostic algorithm, a random forest based on all criteria was calculated.<sup>31</sup> This allowed to quantify each criterion's importance by how much the classification of specimens to AE and CE loses in prediction accuracy if a single criterion is removed from the model.<sup>31</sup> Prediction accuracy was estimated

through cross-validation within the present cohort, for example, leaving one observation out of the estimation step and then predicting its classification. Using a subset of good diagnostic criteria, the optimal decision tree was then determined by recursive partitioning.<sup>32</sup> All statistical analyses were conducted with R (version 3.4.2),<sup>33</sup> and the packages rpart,<sup>34</sup> randomForest,<sup>35</sup> pROC,<sup>36</sup> ROCR,<sup>37</sup> reporttools,<sup>38</sup> ggplot2,<sup>39</sup> partykit,<sup>40</sup> ggparty,<sup>41</sup> and OptimalCutpoints.<sup>42</sup>

## RESULTS

A total of 138 formalin-fixed, paraffin-embedded (FFPE) tissue specimens from 112 patients analyzed at the Department of Pathology and Molecular Pathology, USZ, between 1997 and 2018, were included in this study (Table 1). Given the not definitively subtyped cases of echinococcosis based on clinical data and serology, we first aimed to perform genetic testing in a subset of FFPE echinococcosis specimens to definitively classify these. To this aim, PCR was performed on 48 FFPE tissue samples, of which 42 were informative. On the basis of PCR results, 24 cases were unequivocally classified as AE, and 18 as CE.

We next aimed to test the informative value of IHC for the detection and differentiation of *Echinococcus* spp. in FFPE tissues. In addition to the mAbEm2G11, well established for IHC-S,<sup>17</sup> we applied the hitherto unpublished mAbEmG3, reacting with epitopes of larval stages of both *E. multilocularis* and *E. granulosus* (for validation, see Supplement 1—Table, Supplemental Digital Content 1, <http://links.lww.com/PAS/A841>). IHC-S was first applied to representative specimens of patients with AE and CE, respectively (Fig. 1).

The mAbEmG3 labeled parasitic material including the laminated layer (LL), germinal layer (GL), rostellum, and sheath of the protoscolices of both *E. granulosus* and *E. multilocularis*. Staining patterns of the mAbEm2G11 revealed a strong reactivity with the LL, but not with protoscolices of *E. multilocularis*; no staining was documented

TABLE 1. The Cohort

|              | n (%)  |  |
|--------------|--|--|
|              | <i>Echinococcus multilocularis</i> Infection | <i>Echinococcus granulosus</i> Infection |
| Number       |  |  |
| Total        | 59   | 53                                       |
| Men          | 22 (37.3)                                    | 32 (60.4)                                |
| Women        | 37 (62.7)                                    | 21 (39.6)                                |
| Age (y)      |  |  |
| Minimum      | 19   | 13                                       |
| Maximum      | 79   | 94                                       |
| Average      | 54.6*  | 38.0*                                    |
| Median       | 57   | 35                                       |
| Primary site |  |  |
| Liver        | 55 (93.2)                                    | 45 (84.9)                                |
| Lung         | 2 (3.4)                                      | 0  |
| Soft tissue  | 1 (1.7)                                      | 7 (13.2)                                 |
| Other        | 1 (gall bladder) (1.7)                       | 1 (peritoneum) (1.9)                     |

Main clinicopathologic features of echinococcosis cohort cases.  
\*P < 0.0001 (unpaired 2-tailed t test).

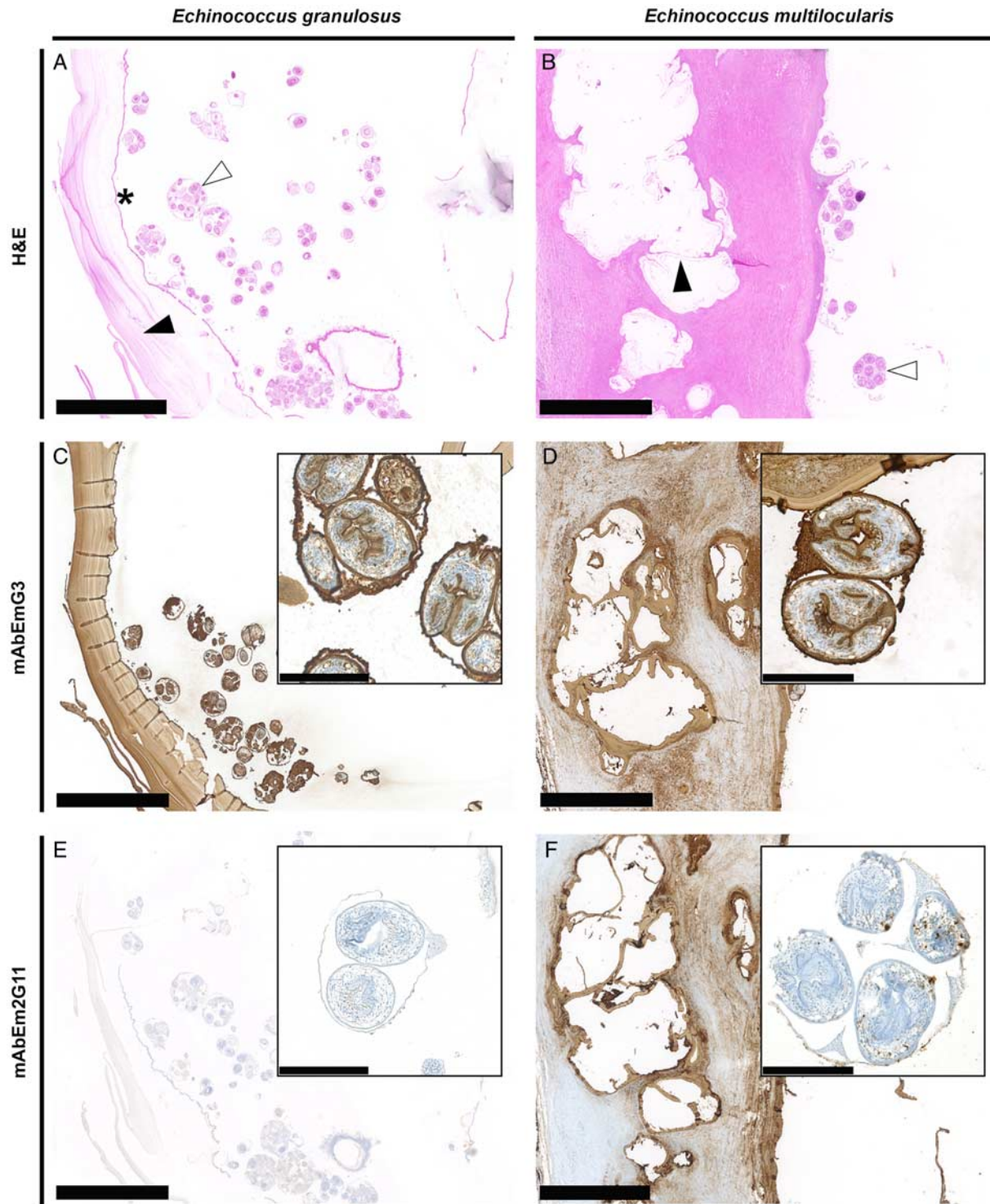


**FIGURE 1.** IHC for the detection of *Echinococcus* spp. A and B, Histomorphology. Typical parasitic material found inside the metacestodes of *Echinococcus granulosus* (A) and *Echinococcus multilocularis* (B) including LLs (black arrowhead), protoscolices (brood capsule marked with white arrowheads), and the GL (asterisk in A). C and D, IHC-S mAbEmG3. The antibody mAbEmG3 stains parasitic material of both *E. granulosus* (C) and *E. multilocularis* (D). Moreover, debris of decayed parasite material is stained in the cyst's surrounding (so-called "SPEMS") (D). E and F, IHC-S mAbEm2G11. Staining patterns of the mAbEm2G11 showing strong reactivity with metacestodes of *E. multilocularis* (F), but negativity in *E. granulosus* metacestodes (E). In contrast to the mAbEm2G11 (F), the mAbEmG3 notably also stains rostellum and tegument of the protoscolex (D). Scale bars (in A–F): 1 mm; insets: 100  $\mu$ m.

**TABLE 2.** Statistical Data Part 1: Continuous Criteria

|                                   | Type of Echinococcosis | Range      | Median | AUC  | 95% CI    | Cutpoint |
|-----------------------------------|------------------------|------------|--------|------|-----------|----------|
| <b>Thickness LL (mm)</b>          | AE                     | 0.05-0.50  | 0.05   | 0.99 | 0.96-1.00 | ≤ 0.15   |
|                                   | CE                     | 0.15-2.10  | 0.60   |      |           | > 0.15   |
| <b>Size of smallest cyst (cm)</b> | AE                     | 0.10-7.00  | 0.10   | 0.97 | 0.93-1.00 | ≤ 0.20   |
|                                   | CE                     | 0.10-20.00 | 4.80   |      |           | > 0.20   |
| <b>Size of largest cyst (cm)</b>  | AE                     | 0.10-10.00 | 1.15   | 0.92 | 0.85-0.98 | ≤ 2.50   |
|                                   | CE                     | 0.10-20.00 | 8.00   |      |           | > 2.50   |
| <b>Thickness of fibrosis (mm)</b> | AE                     | 0.00-3.00  | 0.30   | 0.89 | 0.80-0.96 | ≤ 0.60   |
|                                   | CE                     | 0.00-15.00 | 1.10   |      |           | > 0.60   |
| Lesion size (cm)                  | AE                     | 1.20-20.00 | 8.00   | 0.57 | 0.45-0.69 | —        |
|                                   | CE                     | 0.50-20.00 | 9.00   |      |           | —        |

Criteria informative for differential diagnosis are highlighted in bold letters.  
CI indicates confidence interval; AUC, area under the curve.

using metacestode material from patients with CE. Simultaneous reactivity with both mAbs was regarded as diagnostic for AE, while positivity only for the mAbEmG3 was regarded as diagnostic of CE. Thus, the mAbEmG3 has its value also in confirming the diagnosis of echinococcosis in lesions without any diagnostic morphology (eg, in fine-needle aspirates, necrotic debris, completely fibrotic lesions).

Next, we aimed to evaluate the specificity of its IHC reactivity by testing tissues other than from CE and AE patients with the mAbs. To this aim, tissue of a patient with an *E. vogeli* metacestode infection<sup>43</sup> was incubated with both antibodies. The mAbEmG3 showed an intense staining of the GL, sheath, and rostellum of the protoscolices and weak staining of the LL; no positive staining with the mAbEm2G11 was found (Supplement 2—Fig., Supplemental Digital Content 2, <http://links.lww.com/PAS/A842>). Thus, the IHC-S pattern recapitulated the one observed for *E. granulosus* metacestode tissue, but displayed a slightly weaker staining of the LL of *E. vogeli*. Moreover, 4 different nonechinococcal helminths were investigated with both antibodies (Supplement 3—Fig., Supplemental Digital Content 3, <http://links.lww.com/PAS/A843>). Furthermore, tissues of granulomatous reactions not related to echinococcosis were also incubated with both antibodies (Supplement 4—Fig., Supplemental Digital Content 4, <http://links.lww.com/PAS/A844>). None of these incubations resulted in any positive stain (or even faint cross-reaction). On the basis of the above-described staining patterns, we regarded the mAbEmG3 to be specific for *Echinococcus* spp.

Taking advantage of the 42 genetically confirmed AE or CE cases, we next aimed to determine the sensitivity and specificity of immunostaining for the detection of *Echinococcus* spp. in FFPE tissues. We found that all 24 cases previously diagnosed as AE by PCR, consistently revealed a double-positive IHC-S pattern, that is, mAbEmG3(+)/mAbEm2G11(+), whereas all 18 cases previously identified as CE by PCR, showed the combination of mAbEmG3(+)/mAbEm2G11(−). In summary, the 42 cases revealed 100% accordance between PCR testing and IHC (Fig. 1, Supplement 5A—Fig., Supplemental Digital Content 5, <http://links.lww.com/PAS/A845>). Because of this complete agreement, it formally was not possible to determine Cohen's  $\kappa$ . Statistical simulation of 500 agreement tables revealed that the perfect agreement of the two

diagnostic methods is very unlikely to occur by chance (Supplement 5B—Fig., Supplemental Digital Content 5, <http://links.lww.com/PAS/A845>). Therefore, IHC was considered as powerful as PCR testing for the discrimination between CE and AE.

Given that molecular testing and/or IHC for echinococcosis are not universally available in all pathology laboratories, time-consuming, and expensive, we next sought to test the diagnostic power of an evaluation purely based on morphology. To this aim, cases were assigned to either AE or CE, respectively. On the basis of results of IHC-S, performed on all specimens of our cohort, we were then able to clearly assign all cases to CE or AE. First, a panel of macroscopic and microscopic features was recorded, and evaluated for its informative value to discriminate between CE and AE. A summary of results including a detailed statistical evaluation is shown in Tables 2 and 3.

The size of the entire parasitic lesion was determined macroscopically (Fig. 2), with a median of 8.0 cm in AE, and 9.0 cm in CE, thus showing low power to discriminate between AE and CE. In contrast, the size of the smallest cyst (median CE: 4.8 cm/AE: 0.1 cm), and of the largest cyst (median CE: 8.0 cm/AE: 1.15 cm), both revealed a very good discriminative power. Thus, these parameters can be exploited to differentiate between the two entities (smallest cyst ≤ 2 mm and largest cyst ≤ 25 mm pointing toward AE; smallest cyst > 2 mm and largest cyst > 25 mm pointing toward CE). Likewise, the number of cysts within a lesion can be utilized: The number of cysts was divided into two categories: “up to 9 cysts” versus “10 and more cysts.” Using “10 and more cysts” as an indicator for AE, and “9 and less cysts” as an indicator for CE, showed both high sensitivity and specificity, making the number of cysts a powerful diagnostic test.

*E. granulosus* cysts include a surrounding rim of fibrosis, which usually is macroscopically visible as a light beige zone (Fig. 2A). This fibrotic rim reflects the host reaction, and is not part of the parasite tissue (Fig. 3C). The thickness of the pericystic fibrosis (adventitial layer, AL), as determined on elastica van Gieson stains, showed a median of 1.10 mm in the cysts of CE. In contrast, all individual *E. multilocularis* metacestode vesicles were surrounded by a lean fibrotic rim. As the lesions frequently displayed central

**TABLE 3.** Statistical Data Part 2: Categorical Criteria

|                                | Type of Echinococcosis | Diagnostic Criterion | Sensitivity | 95% CI    | Specificity | 95% CI    |
|--------------------------------|------------------------|----------------------|-------------|-----------|-------------|-----------|
| No. cysts                      | AE                     | > 9                  | <b>0.95</b> | 0.85-0.99 | <b>0.90</b> | 0.76-0.97 |
|                                | CE                     | ≤ 9                  |             |           |             |           |
| Striation LL                   | AE                     | Weak                 | <b>0.89</b> | 0.78-0.96 | <b>0.98</b> | 0.87-1.00 |
|                                | CE                     | Moderate-strong      |             |           |             |           |
| Vital protoscolices            | AE                     | Absent               | <b>0.97</b> | 0.88-1.00 | 0.30        | 0.17-0.47 |
|                                | CE                     | Present              |             |           |             |           |
| Calcification of protoscolices | AE                     | Absent               | <b>0.95</b> | 0.86-0.99 | 0.05        | 0.01-0.17 |
|                                | CE                     | Present              |             |           |             |           |
| Calcification of LL            | AE                     | Absent               | <b>0.91</b> | 0.81-0.97 | 0.03        | 0.00-0.13 |
|                                | CE                     | Present              |             |           |             |           |
| Necrosis                       | AE                     | Present              | <b>0.85</b> | 0.73-0.93 | 0.25        | 0.13-0.41 |
|                                | CE                     | Absent               |             |           |             |           |
| Generally chronic inflammation | AE                     | No-little            | 0.80        | 0.67-0.89 | 0.25        | 0.13-0.41 |
|                                | CE                     | Much                 |             |           |             |           |
| Lymphoplasmocytic inflammation | AE                     | No-little            | 0.80        | 0.67-0.89 | 0.25        | 0.13-0.41 |
|                                | CE                     | Much                 |             |           |             |           |
| Follicular inflammation        | AE                     | Absent               | 0.76        | 0.63-0.86 | 0.25        | 0.13-0.41 |
|                                | CE                     | Present              |             |           |             |           |
| Calcification of pericyst      | AE                     | Absent               | 0.69        | 0.55-0.80 | 0.20        | 0.09-0.36 |
|                                | CE                     | Present              |             |           |             |           |
| Calcospherites                 | AE                     | Present              | 0.63        | 0.49-0.75 | <b>0.85</b> | 0.70-0.94 |
|                                | CE                     | Absent               |             |           |             |           |
| Ghost protoscolices            | AE                     | Absent               | 0.53        | 0.39-0.66 | 0.73        | 0.56-0.85 |
|                                | CE                     | Present              |             |           |             |           |
| General calcification          | AE                     | Much                 | 0.51        | 0.37-0.64 | <b>0.90</b> | 0.76-0.97 |
|                                | CE                     | No-little            |             |           |             |           |
| GL                             | AE                     | Absent               | 0.51        | 0.37-0.64 | <b>0.85</b> | 0.70-0.94 |
|                                | CE                     | Present              |             |           |             |           |
| Neutrophilic inflammation      | AE                     | Much                 | 0.49        | 0.36-0.63 | <b>0.85</b> | 0.70-0.94 |
|                                | CE                     | No-little            |             |           |             |           |
| Foreign body reaction          | AE                     | Present              | 0.46        | 0.33-0.59 | 0.65        | 0.48-0.79 |
|                                | CE                     | Absent               |             |           |             |           |
| Calcification of detritus      | AE                     | Absent               | 0.43        | 0.30-0.57 | 0.25        | 0.13-0.41 |
|                                | CE                     | Present              |             |           |             |           |
| Generally active inflammation  | AE                     | Present              | 0.42        | 0.30-0.56 | <b>0.88</b> | 0.73-0.96 |
|                                | CE                     | Absent               |             |           |             |           |
| Eosinophilic inflammation      | AE                     | Present              | 0.42        | 0.30-0.56 | 0.75        | 0.59-0.87 |
|                                | CE                     | Absent               |             |           |             |           |

Criteria informative for differential diagnosis are highlighted in bold letters. For criteria with high specificity and/or sensitivity, the values are highlighted in bold numbers. CI indicates confidence interval.

necrotic areas with numerous confluent cysts and concomitant fibrotic reaction, the thickness of individual cysts was not measured inside the lesion, but rather in the outer part containing intact single cysts showing a median of 0.3 mm in cysts of AE (Fig. 3D). The thickness of the pericystic fibrosis was shown to be a powerful diagnostic criterion to differentiate between AE and CE. Infections with both parasites induced an inflammatory reaction in the tissue adjacent to the cystic lesions. In intact cysts, the components, and intensity of the inflammatory infiltrate (lymphoplasmocellular, active, follicular, foreign body reaction, eosinophilic, generally chronic, and generally active) showed very low sensitivity and/or specificity (Table 3). Thus, the cellular composition of the inflammatory reaction was not considered a criterion suitable to discriminate between AE and CE.

Parasitic lesions in both CE and AE patients constitute a cell-free carbohydrate-protein layer designated as LL. The LLs of *E. granulosus* and *E. multilocularis* obviously differ with respect to their shape and thickness (Figs. 3E, F). The

LL of *E. granulosus* was merely thick (median 0.6 mm) and showed a sharply demarcated striation—reminiscent of the creasing of a vinyl—as well as a rather eosinophilic coloration in H&E stain. In contrast, the LL of *E. multilocularis* displayed a thin (median 0.05 mm), in HE stain rather pale and blueish colored membrane with no prominent creasing—reminiscent of a watercolor painting. The morphologic criteria “thickness of the LL” showed a very high power to discriminate between AE and CE (a thickness ≤0.15 mm pointing toward AE/>0.15 mm pointing toward CE). Moreover, the thickness of the LL turned out to be the single best diagnostic criterion for differentiating between the two parasites. The striation pattern was dichotomized into 2 categories (weak striation vs. moderate-strong striation). Using a “moderate to strong striation” as an indicator of CE and a “weak striation” as an indicator of AE showed high sensitivity and specificity. Thus, striation proved to be a further diagnostically valuable criterion.

Although the presence of a nucleated GL had been reported to be restricted to CE,<sup>19</sup> we detected a GL in 50.8% of

Downloaded from http://ajsp.ajsp.com/ by BNDM5ePHKav1ZEumt1QIN4a+kJLhEz7gbsHh04XM10hOywCX1AV nYQpI1QH3D3D00dRv7TVSf14C3VVC1y0abg9QZXdG5j2MwIzLel= on 03/28/2023

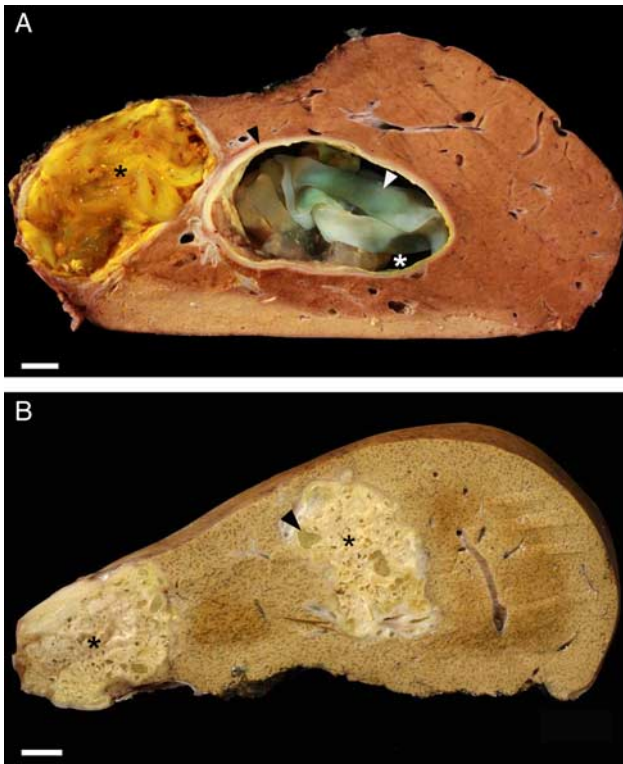


**FIGURE 2.** Diagnostic criteria for differentiation of CE and AE: macroscopy. **A**, Liver specimen with 2 large cysts of *Echinococcus granulosus* metacestodes. One cyst is necrotic (black asterisk), the other presumably vital (white asterisk). Inside the large cyst, parts of the LL are visible (white arrowhead). The cystic lesions are surrounded by fibrous capsule (pericystic fibrosis/AL; black arrowhead), which is produced by the host. **B**, Hemihepatectomy specimen with *Echinococcus multilocularis* infection revealing 2 spongy solidifications (black asterisks) comprising conglomerates of tiny cysts (the largest marked by the black arrowhead). Because of its small size, the LL cannot be identified macroscopically. In contrast to CE, AE does not show a clear-cut margin by a prominent perilesional fibrotic zone. Scale bars: 1 cm.

AE cases. Moreover, the detectability of protoscolices in AE had been controversially discussed.<sup>19,20,44</sup> We detected viable (28.3% in CE vs. 1.7% in AE, Fig. 1) and decaying (ghost) protoscolices (70.4% in CE vs. 45.8% in AE) in both diseases. Thus, neither the presence of a GL nor that of protoscolices proved to be a useful diagnostic criterion.

The lesions of both *Echinococcus* spp. contain not only well-defined parasitic structures, but also detritus and antigenic remnants. In *E. multilocularis* metacestodes, they have been visualized by IHC-S with the mAbEm2G11, and designated as “SPEMS” (small particles of *E. multilocularis*).<sup>17</sup> SPEMS were detectable not only within the cyst but also in the liver tissue surrounding the cysts. The SPEMS’ staining pattern was not only recapitulated with mAbEmG3, but displayed even a stronger positivity compared with the mAbEm2G11. Staining all of these lesions with mAbEmG3 not only confirmed this finding, but the staining pattern also was more pronounced

(Supplement 6A, B—Fig., Supplemental Digital Content 6, <http://links.lww.com/PAS/A846>). Although the LL of *E. granulosus* is considered an important immune evasion structure protecting the GL from the host’s defense, staining of pericystic tissue with mAbEmG3 surprisingly revealed a positive reaction in the pericystic tissue showing small particles of *E. granulosus* (SPEGS; Supplement 6C—Fig., Supplemental Digital Content 6, <http://links.lww.com/PAS/A846>). We could not find any obvious difference in the amount or intensity of pericystic antigenic material in AE versus CE using mAbEmG3.

Besides those discussed above, further criteria were tested as potential discriminators including necrosis, calciferous corpuscles, or calcification in pericyst/LL/protoscolices/necrotic debris. However, none of these proved powerful in discriminating between CE versus AE. Using classical ROC analysis, we identified six histologic criteria as powerful tools discriminating between CE and AE. These are the (i) size of smallest cyst, (ii) thickness of the LL, (iii) size of largest cyst, (iv) striation of the LL, (v) number of cysts, and (vi) thickness of the pericystic fibrosis. This was confirmed by the fitting of a random forest using all criteria and identifying the same 6 histologic criteria as most influential in an importance plot (Fig. 4).

Next, we sought to develop an easy to use and robust algorithm based on the histopathologic criteria analyzed in this study, which allows the surgical pathologist to differentiate between CE and AE. In conjunction with serologic findings, IHC, and genetic (PCR-based) testing, the histomorphologic findings of our study were integrated into an algorithm that guides the diagnosis and differential diagnosis of echinococcosis (Fig. 5). This approach enabled us to unequivocally classify all cases of our cohort as either CE or AE, respectively, including the 54 cases that before re-evaluation for this study had been assigned as “echinococcosis NOS.” Of note, determining the optimal tree using the six identified histologic criteria, already a combination of only two of these, that is, thickness of LL and thickness of pericystic fibrosis (AL), allowed us to diagnose with an estimated prediction accuracy of 95% in our cohort (Supplement 7—Fig., Supplemental Digital Content 7, <http://links.lww.com/PAS/A847>).

Finally, we applied the tools and the newly developed diagnostic algorithm on difficult to diagnose cases: (1) A 55-year-old female breast cancer patient with a cystic liver lesion suspicious of liver metastasis (Figs. 6A–C). (2) A 37-year-old male patient who presented with cystic bone lesions of unknown nature in the lumbosacral region, surrounded by pericystic bone destruction (Figs. 6D–F). (3) A 78-year-old female patient with metastasizing ovarian cancer, and an incidental finding of a cystic lesion on liver surgery (Figs. 6G–I). Although neither histology nor initial serologic testing was diagnostic, we were able to make the final diagnosis of echinococcosis in all 3 cases by applying IHC-S. Thus, combined IHC-S introduced here is useful for reliably diagnosing (mAbEmG3) and subsequently subtyping (mAbEm2G11) echinococcosis, particularly in clinically unexpected cases and those with equivocal or lacking serologic results.

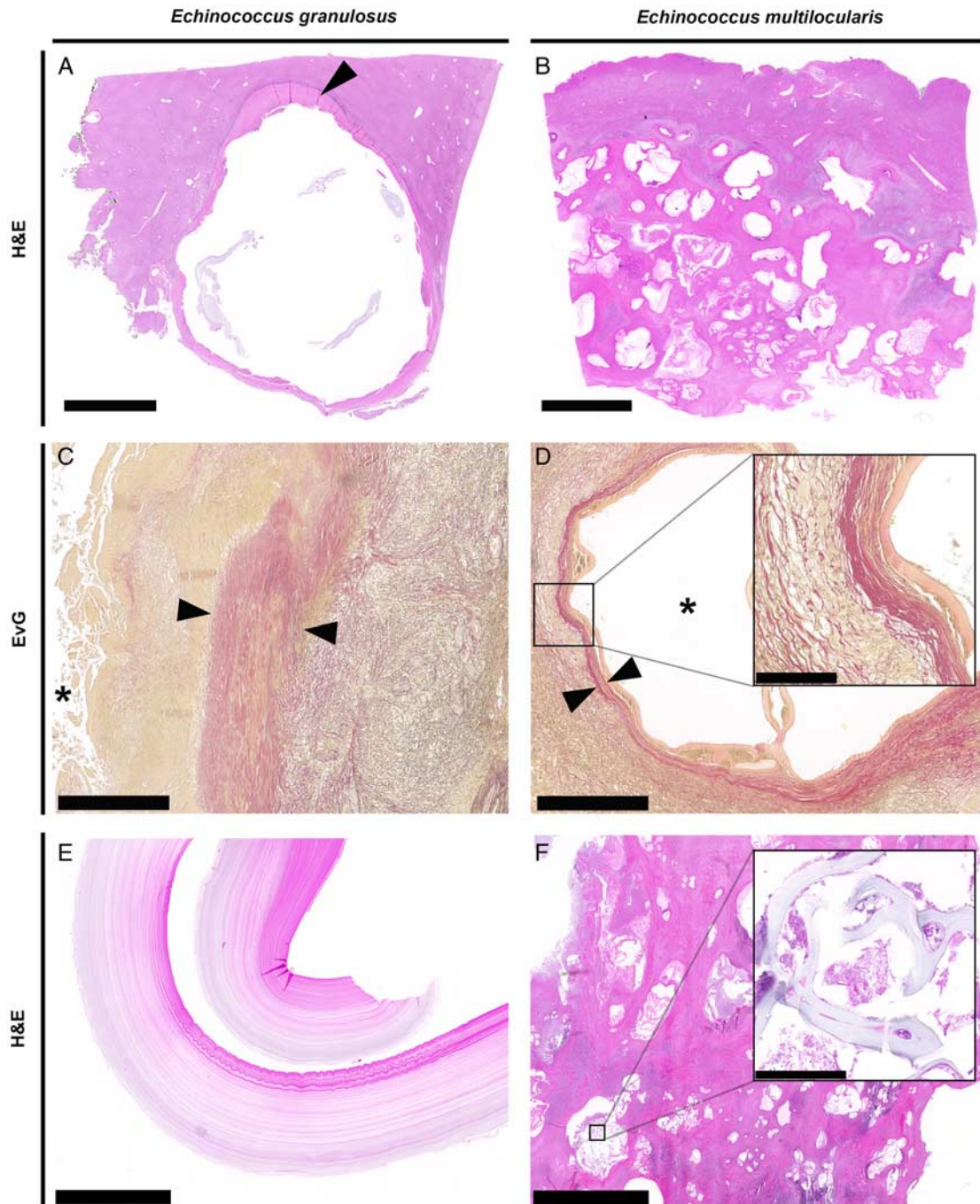


**FIGURE 3.** Diagnostic criteria for differentiation of CE and AE: Histology. Characteristic histologic patterns comparing CE (A) with AE (B). A, A single larger cyst with a fibrotic rim (AL, arrowhead) and liver tissue. Inside the cyst, some parts of the LL are visible. B, Polycystic lesion with lots of small, polymorphous, and partly conglomerated cysts. Although the center frequently is necrotic and fibrotic, the single cyst at the periphery is not accompanied by a broad fibrotic rim. Contorted parts of the LL are present in the lumina of some of the cysts. C and D, Pericystic fibrosis. Cysts of *Echinococcus granulosus* metacestodes constantly display a significantly broader fibrotic capsule, known as cyst capsule, pericyst, or AL (between the two arrowheads, elastica van Gieson stain) (C) compared with those of *Echinococcus multilocularis* (D). Cyst lumina marked with an asterisk. E and F, Morphology of LL. E, Thick LL of *E. granulosus* cysts with a rather reddish appearance in H&E staining with typically prominent striation. F, Lesion of *E. multilocularis* metacestodes with numerous small cysts, partly filled with thin conglomerates of LL. The inset shows the thin LL with a more or less bluish-clear aspect in H&E staining, lacking a prominent striation even at higher magnification. Note that (E) and (F) are recorded in the same magnification. Scale bars: A and B: 5 mm, C and D: 500  $\mu$ m, E and F: 2.5 mm, all insets: 100  $\mu$ m.



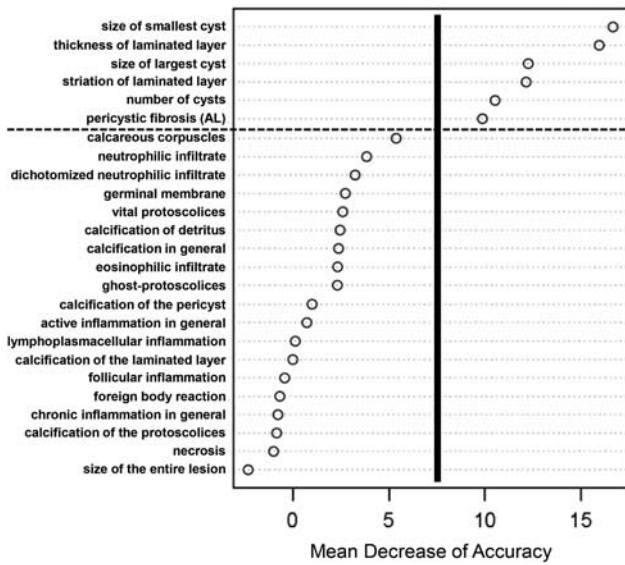


**FIGURE 4.** Change of prediction accuracy. The plot shows the mean decrease of the prediction accuracy if excluding single assessment criteria. The first six criteria are the most valuable ones (the most meaningful are size of the smallest cyst and thickness of the LL). Two further criteria, that is, the detection of calcospherites and of a granulocytic inflammatory response have a tendency to be useful. Thus, they potentially can be used as additional corroborative criteria. For better visualization, vertical and horizontal lines separate the 6 powerful diagnostic criteria (on the right side) from the rest, the latter showing a lesser decrease of prediction accuracy.

**DISCUSSION**

AE and CE, parasitic diseases with significant global health burden, are recently increasingly recognized in many parts of the world including North America.<sup>2,7,45</sup> Although the liver is the organ most affected by both CE (68.8%) and AE (99.0%),<sup>9,10,20</sup> the course of the diseases, their prognoses, and patients' management decisively differ between the two.<sup>10</sup> Treatment of CE comprises a variety of approaches including surgical procedures (pericystectomy/cystectomy, liver segment resection etc.) combined with temporary treatment with albendazole, percutaneous treatments to destroy the GL or to evacuate the entire endocyst, and mostly short-term treatment with antiparasitic drugs.<sup>20,46</sup> In contrast, for AE, long-term or even lifelong drug treatment and/or radical resection in combination with a drug treatment at least for 2 years are recommended.<sup>20</sup> Thus, discriminating CE versus AE is a prerequisite for the optimal therapeutic management. Therefore, a putative diagnosis based on imaging and serology should be confirmed by histopathology, optionally supplemented by PCR and/or IHC, to avoid a diagnosis of "echinococcosis, NOS."

Thus, there is clearly a need to identify (histo-)pathologic criteria, which allow to reliably discriminate between CE and AE. However, a systematic and thorough (histo-)pathologic description of echinococcosis on a substantial number of cases was still awaiting. For example, the discrimination between CE and AE was restricted to the differences in the number of cysts or the macroscopic

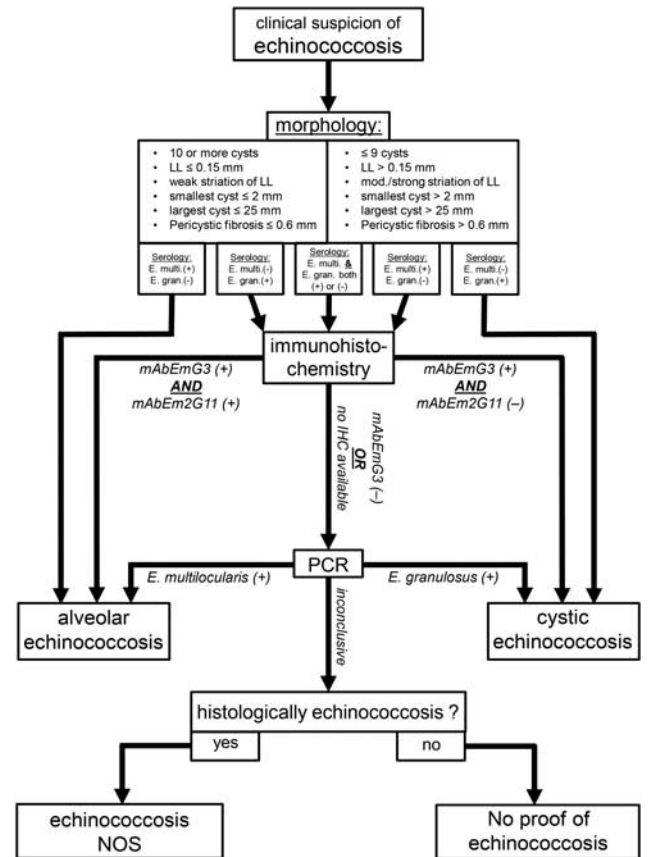


**FIGURE 5.** A diagnostic algorithm for echinococcosis. On the basis of clinical suspicion of echinococcosis (eg, by ultrasound findings), the combination of the congruency of the 6 depicted histologic criteria and the serologic findings in most cases can lead to the correct diagnosis. In equivocal cases, a stepwise approach can be followed by integrating IHC, followed by molecular testing. In case histology, IHC, and PCR testing collectively are inconclusive, the decision has to be made, on the basis of conventional histology, as to whether or not there is substantial clue for echinococcosis, then denominated as "echinococcosis, NOS" versus "no proof of echinococcosis."

growth type.<sup>47</sup> Moreover, the metacestode stage of *E. granulosus* has been described as a slowly growing cystic mass, in contrast to metacestode of *E. multilocularis* composed of a conglomerate with a cancer-like invasive growth.<sup>48</sup> However, a detailed (histo-)pathologic description of the different cyst components of both *Echinococcus* spp. was lacking.

The comprehensive and statistically underpinned analysis of a cohort of >100 echinococcosis surgical specimens performed in this study resulted in several findings that are not in line with the current textbook knowledge and go beyond what has been reported in previous studies.<sup>44</sup> For example, criteria claimed to be specific for CE, that is, fully developed protoscolices and the GL,<sup>19</sup> were also found in *E. multilocularis* metacestode tissue in our observations.

Several histopathologic changes were reported to differ between *E. granulosus* and *E. multilocularis* lesions,<sup>19,20,47,48</sup>

Downloaded from http://ajsp.ajsp.com/ by guest on 03/28/2023

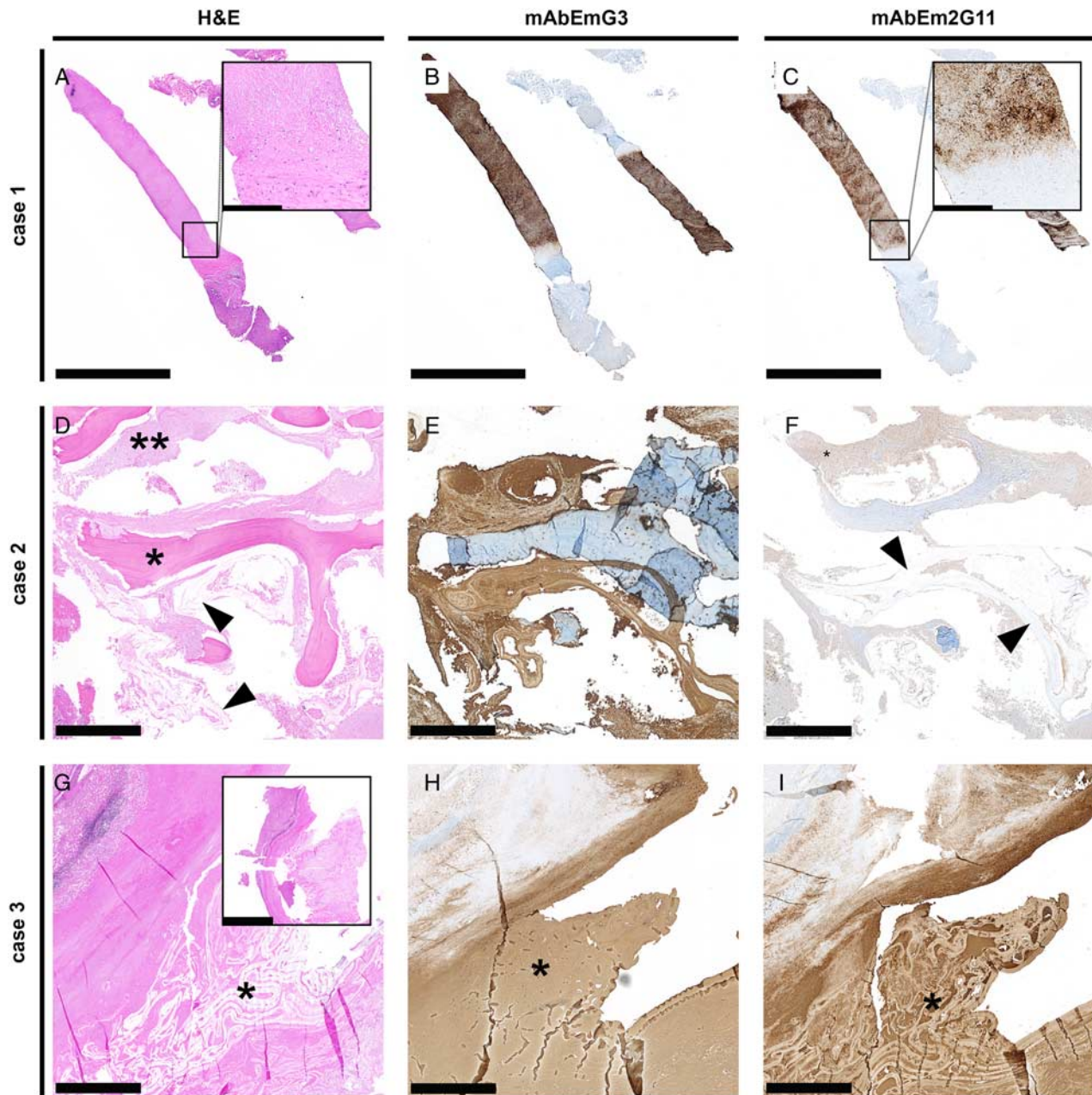


**FIGURE 6.** Three challenging cases illustrating the diagnostic power of IHC. A–C, Case 1 of a 55-year-old female patient with a history of recent breast cancer. Biopsy of a suspected liver metastasis revealing liver tissue bordered by a short fibrotic zone and plenty of necrosis without any structured morphology (A). Strong positivity of necrotic debris for mAbEmG3 (B) and mAbEm2G11 (C), allowing to confidently diagnose the lesion as an AE. D–F, Case 2 of a 37-year-old male patient with an unclear cystic bone lesion in the lumbosacral region. Histology (D) reveals lamellar bone tissue (asterisk), surrounded by necrotic debris (double asterisk) and lots of thin LL (black arrowheads). Debris and LL strongly react with the mAbEmG3 (E), but not with the mAbEm2G11 (F), thus pointing to an *Echinococcus granulosus* infection. G–I, Case 3 of a 78-year-old female patient with metastasizing papillary ovarian cancer. Incidental finding of a cystic liver lesion during surgery. The lesion consists of a single cyst with pericyclic fibrosis, morphologically reminiscent of an *E. granulosus* cyst (G, inset). Within the cysts’ lumen, numerous thin LL are detectable (G, asterisk). LL, debris, and parts of the surrounding tissue stain strongly for mAbEmG3 (H) and mAbEm2G11 (I), indicative of AE. LL is marked with an asterisk. Scale bars: A–C: 2.5 mm, insets in A and C: 250  $\mu$ m, D–F: 500  $\mu$ m, G–I: 1 mm, inset in G: 5 mm.

and thus proposed as discriminating criteria. However, these studies did not include any statistical evaluation of individual (or combined) criteria for their discriminative value. We,

here, identified six statistical validated pathologic criteria, which allow us to confidently discriminate between CE and AE (Tables 2, 3). Moreover, we have demonstrated already

that two histopathologic criteria, that is, the thickness of the LL and the thickness of the pericystic fibrosis of a single cyst (AL), allowed us to discriminate between CE and AE with an estimated prediction accuracy of 95% in our cohort (Supplement 7—Fig., Supplemental Digital Content 7, <http://links.lww.com/PAS/A847>). A central result of the present study is the new and robust diagnostic algorithm, which is easily applicable in daily practice to differentiate between CE and AE. Thus, we consider already the histology-based part of the diagnostic algorithm (Fig. 5) to be powerful for the differentiation between CE and AE.

Another central result of the present study is the validation of the novel mAbEmG3 directed against *Echinococcus spp.* and its implementation for routine use. The evaluation clearly documented the genus specificity of the mAbEmG3, reacting with both structural antigens and with cyst fluid of both *Echinococcus spp.* Interestingly, mAbEmG3 reacts with mAbEm2G11 affinity purified Em2 antigen and with *E. granulosus* antigens. This *Echinococcus spp.* specificity makes the mAbEmG3 a powerful ancillary tool in different diagnostic settings. IHC-S with this antibody can be exploited to reliably diagnose echinococcosis even in the complete or partial absence of clearly identifiable morphologic criteria in tissue sections—as illustrated in the cases shown in Figure 6. We demonstrated that a combined IHC-S approach with both antibodies is equally specific as, and occasionally even more sensitive than, the previous gold standard of PCR-based genetic testing. On the basis of these observations, and given that we did not observe a single case completely void of any immunoreactivity, we concluded that—although a double-negative staining result cannot ultimately exclude echinococcosis—it is suggestive of an underlying pathology other than echinococcal infection.

Remarkably, similar to the mAbEm2G11, the mAbEmG3 also allowed us to detect—presumably pericystic—decayed parasitic material, representing small particles of *E. multilocularis*, the so-called “SPEMS.”<sup>17</sup> We demonstrated these antigenic particles not only in AE cases, but also in cases of CE, indicating that “SPEMS” are not restricted to AE. Thus, we propose to term these small antigenic particles in CE as SPEGS. The presence of this particular immunogenic material might not only be useful in several diagnostic scenarios such as cytologies of aspirates, but also be relevant for understanding the host’s immune reaction against the parasite.

In summary, the present study improves our knowledge on the histopathology of echinococcosis. We have challenged several statements on echinococcosis, identified robust histopathologic criteria as discriminators between CE and AE, and introduced a highly sensitive and specific IHC panel. We expect our findings to improve histopathologic diagnosis, thus impacting on patients’ management of echinococcosis.

#### ACKNOWLEDGMENTS

The authors thank Christiane Mittmann, Fabiola Prutek, André Fitsche, Marcel Glöckler, Norbert Wey,

Susanne Dettwiler, and Martina Storz and her team, for their excellent technical support.

#### REFERENCES

- Budke CM, Deplazes P, Torgerson PR. Global socioeconomic impact of cystic echinococcosis. *Emerg Infect Dis.* 2006;12:296–303.
- Deplazes P, Rinaldi L, Alvarez Rojas CA, et al. Global distribution of alveolar and cystic echinococcosis. *Adv Parasitol.* 2017;95:315–493.
- Agudelo Higueta NI, Brunetti E, McCloskey C. Cystic echinococcosis. *J Clin Microbiol.* 2016;54:518–523.
- Kern P. Clinical features and treatment of alveolar echinococcosis. *Curr Opin Infect Dis.* 2010;23:505–512.
- Moro P, Schantz PM. Cystic echinococcosis in the Americas. *Parasitol Int.* 2006;55(suppl):S181–S186.
- Trotz-Williams LA, Mercer NJ, Walters JM, et al. Public health follow-up of suspected exposure to *Echinococcus multilocularis* in Southwestern Ontario. *Zoonoses Public Health.* 2017;64:460–467.
- Taxy JB, Gibson WE, Kaufman MW. Echinococcosis: unexpected occurrence and the diagnostic contribution of routine histopathology. *Am J Surg Pathol.* 2017;41:94–100.
- Alvarez Rojas CA, Mathis A, Deplazes P. Assessing the contamination of food and the environment with taenia and *Echinococcus* eggs and their zoonotic transmission. *Curr Clin Microbiol Rep.* 2018;5:154–163.
- Eckert J, Deplazes P. Biological, epidemiological, and clinical aspects of echinococcosis, a zoonosis of increasing concern. *Clin Microbiol Rev.* 2004;17:107–135.
- Kern P, Menezes da Silva A, Akhan O, et al. The echinococcoses: diagnosis, clinical management and burden of disease. *Adv Parasitol.* 2017;96:259–369.
- Kratzer W, Gruener B, Kaltenbach TE, et al. Proposal of an ultrasonographic classification for hepatic alveolar echinococcosis: *Echinococcus multilocularis* Ulm classification-ultrasound. *World J Gastroenterol.* 2015;21:12392–12402.
- Graeter T, Kratzer W, Oeztuerk S, et al. Proposal of a computed tomography classification for hepatic alveolar echinococcosis. *World J Gastroenterol.* 2016;22:3621–3631.
- Eckert J, Gemmel MA, Meslin FX, et al. *WHO/OIE Manual on Echinococcosis in Humans and Animals: a Public Health Problem of Global Concern.* Paris, France: World Organization for Animal Health; 2001:265.
- Schweiger A, Grimm F, Tanner I, et al. Serological diagnosis of echinococcosis: the diagnostic potential of native antigens. *Infection.* 2012;40:139–152.
- Siles-Lucas M, Casulli A, Conraths FJ, et al. Laboratory diagnosis of *Echinococcus spp.* in human patients and infected animals. *Adv Parasitol.* 2017;96:159–257.
- Bebezov B, Mamashev N, Umetaliev T, et al. Intense focus of alveolar echinococcosis, South Kyrgyzstan. *Emerg Infect Dis.* 2018;24:1119–1122.
- Barth TF, Herrmann TS, Tappe D, et al. Sensitive and specific immunohistochemical diagnosis of human alveolar echinococcosis with the monoclonal antibody Em2G11. *PLoS Negl Trop Dis.* 2012;6:e1877.
- Marty AM, Johnson AK, Neafie RC. Hydatidosis (echinococcosis). In: Meyers WM, Neafie RC, Marty AM, Wear DJ, eds. *Pathology of Infectious Diseases.* Washington, DC: Armed Forces Institute of Pathology; 2000:145–164.
- Burt A, Ferrel L, Hubscher S, et al. *Mac Sween's Pathology of the Liver*, 6th edition. Edinburgh, UK; New York, NY: Churchill Livingstone/Elsevier; 2012.
- Brunetti E, Kern P, Vuitton DA, et al. Expert consensus for the diagnosis and treatment of cystic and alveolar echinococcosis in humans. *Acta Trop.* 2010;114:1–16.
- Hulsmeier AJ, Gehrig PM, Geyer R, et al. A major *Echinococcus multilocularis* antigen is a mucin-type glycoprotein. *J Biol Chem.* 2002;277:5742–5748.
- Deplazes P, Gottstein B. A monoclonal antibody against *Echinococcus multilocularis* Em2 antigen. *Parasitology.* 1991;103(pt 1):41–49.

23. Joekel DE, Deplazes P. Optimized dexamethasone immunosuppression enables *Echinococcus multilocularis* liver establishment after oral egg inoculation in a rat model. *Exp Parasitol*. 2017;180:27–32.
24. Boege Y, Malehmir M, Healy ME, et al. A dual role of caspase-8 in triggering and sensing proliferation-associated DNA damage, a key determinant of liver cancer development. *Cancer Cell*. 2017;32:342.e10–359.e10.
25. Lenggenhager D, Gouttenoire J, Malehmir M, et al. Visualization of hepatitis E virus RNA and proteins in the human liver. *J Hepatol*. 2017;67:471–479.
26. Stieger C, Hegglin D, Schwarzenbach G, et al. Spatial and temporal aspects of urban transmission of *Echinococcus multilocularis*. *Parasitology*. 2002;124:631–640.
27. Stefanic S, Shaikenov BS, Deplazes P, et al. Polymerase chain reaction for detection of patent infections of *Echinococcus granulosus* (“sheep strain”) in naturally infected dogs. *Parasitol Res*. 2004;92:347–351.
28. Trachsel D, Deplazes P, Mathis A. Identification of taeniid eggs in the faeces from carnivores based on multiplex PCR using targets in mitochondrial DNA. *Parasitology*. 2007;134:911–920.
29. Cohen J. A coefficient of agreement for nominal scales. *Educ Psychol Meas*. 1960;20:37–46.
30. Kirkwood BR, Sterne JA. *Essential Medical Statistics*. Hoboken, New Jersey: John Wiley & Sons; 2010.
31. Breiman L. Random Forests. *Mach Learn*. 2010;45:5–32.
32. Breiman L, Friedman J, Stone CJ, et al. *Classification and Regression Trees*. Milton Park, UK: Taylor & Francis; 1984.
33. R Core Team. *R: A Language and Environment for Statistical Computing*. Vienna, Austria: R Foundation for Statistical Computing; 2017.
34. Therneau TM, Atkinson B. rpart: recursive partitioning and regression trees; 2018.
35. Liaw A, Wiener M. Classification and regression by randomForest. *R News*. 2002;2:18–22.
36. Robin X, Turck N, Hainard A, et al. pROC: an open-source package for R and S+ to analyze and compare ROC curves. *BMC Bioinformatics*. 2011;12:77.
37. Sing T, Sander O, Beerenwinkel N, et al. ROCR: visualizing classifier performance in R. *Bioinformatics*. 2005;21:3940–3941.
38. Ruffibach K. reporttools: R functions to generate LaTeX tables of descriptive statistics. *J Stat Softw*. 2009;31:1–7.
39. Wickham H. *ggplot2: Elegant Graphics for Data Analysis*. New York, NY: Springer-Verlag; 2016.
40. Hothorn T, Zeileis A. partykit: a modular toolkit for recursive partytioning in R. *J Mach Learn Res*. 2015;16:3905–3909.
41. Borkovec M, Madin N. ggparty: ‘ggplot’ visualizations for the ‘partykit’ Package. R package, version 1.0.0; 2019.
42. López-Ratón M, Rodríguez-Álvarez MX, Cadarso-Suárez C, et al. OptimalCutpoints: an R package for selecting optimal cutpoints in diagnostic tests. *J Stat Softw*. 2014;61:1–36.
43. Stijnis K, Dijkmans AC, Bart A, et al. *Echinococcus vogeli* in immigrant from Suriname to the Netherlands. *Emerg Infect Dis*. 2015;21:528–530.
44. Ammann RW, Eckert J. Cestodes. *Echinococcus*. *Gastroenterol Clin North Am*. 1996;25:655–689.
45. Massolo A, Liccioli S, Budke C, et al. *Echinococcus multilocularis* in North America: the great unknown. *Parasite*. 2014;21:73.
46. Buttenschoen K, Carli Buttenschoen D. *Echinococcus granulosus* infection: the challenge of surgical treatment. *Langenbecks Arch Surg*. 2003;388:218–230.
47. Milner DA, Pecora N, Solomon I, et al. *Diagnostic Pathology: Infectious Diseases*, 1st edition. Philadelphia, PA: Elsevier; 2015.
48. Kradin RL. *Diagnostic Pathology of Infectious Disease*, 1st edition. Philadelphia, PA: Saunders Elsevier; 2010.